Analyst

Accepted Manuscript

This is an *Accepted Manuscript*, which has been through the RSC Publishing peer review process and has been accepted for publication.

Accepted Manuscripts are published online shortly after acceptance, which is prior to technical editing, formatting and proof reading. This free service from RSC Publishing allows authors to make their results available to the community, in citable form, before publication of the edited article. This *Accepted Manuscript* will be replaced by the edited and formatted *Advance Article* as soon as this is available.

To cite this manuscript please use its permanent Digital Object Identifier (DOI®), which is identical for all formats of publication.

More information about *Accepted Manuscripts* can be found in the **Information for Authors**.

Please note that technical editing may introduce minor changes to the text and/or graphics contained in the manuscript submitted by the author(s) which may alter content, and that the standard **Terms & Conditions** and the **ethical guidelines** that apply to the journal are still applicable. In no event shall the RSC be held responsible for any errors or omissions in these *Accepted Manuscript* manuscripts or any consequences arising from the use of any information contained in them.

Cite this: DOI: 10.1039/c0xx00000x

www.rsc.org/xxxxxx

ARTICLE TYPE

Highly enhanced electrochemiluminescence based on pseudo triple-enzyme cascade catalysis and in situ generate co-reactant for thrombin detection

Lijuan Xiao, Yaqin Chai*, Ruo Yuan*, Haijun Wang and Lijuan Bai

Received (in XXX, XXX) Xth XXXXXXXXX 20XX, Accepted Xth XXXXXXXXX 20XX
DOI: 10.1039/b000000x

In this work, a novel pseudo triple-enzyme cascade catalysis amplification strategy was employed to fabricate a highly sensitive electrochemiluminescence (ECL) aptasensor for thrombin (TB) detection. The signal amplification of the proposed aptasensor was based on the synergistic catalysis of glucose dehydrogenase (GDH) and hemin/G-quadruplex to generate co-reactant in situ for ECL of peroxydisulfate. Gold nanorods conjugated with GDH and hemin/G-quadruplex was used as secondary aptamer bioconjugate (TBA II) in this aptasensor. TB was sandwiched between TBA II and thiol-terminated TB aptamer which self-assembled on gold nanoparticles modified electrode. The pseudo triple-enzyme cascade catalysis was completed as follows: Firstly, GDH could effectively catalyze the oxidation of glucose to gluconolatone, coupling with the reduction of β-nicotinamide adenine dinucleotide hydrate (NAD^+) into β-nicotinamide adenine diuncleotide hydrogen (NADH). Then, the hemin/G-quadruplex acted as NADH oxidase, could rapidly oxidize NADH into NAD^+ accompanying with the generation of H_2O_2. Simultaneously, the hemin/G-quadruplex served as the horseradish peroxidase (HRP)-mimicking DNAzyme further catalyzed the reduction of H_2O_2 to generate O_2 in situ. Then the produced O_2 acted as the co-reactant of peroxydisulfate, resulting in significant ECL signal amplification and highly sensitive ECL detection. The proposed aptasensor showed a wide linear range of 0.0001 nM-50 nM with a low detection limit of 33 fM (S/N = 3) for TB determination. The present work demonstrated that the novel strategy had great advantages in sensitivity, selectivity and reproducibility, which held a new promise for highly sensitive bioassays applied in clinical detection.

Introduction

Electrochemiluminescent (ECL), a light emission motivated by the high-energy electron transfer reaction, has become an important and powerful analytical tool in environmental pollutant determination, clinical analysis and immunoassays[1-3]. Quantum dots, Ru complex, luminol and its derivatives as common ECL regents, have been widely used to construct ECL biosensors[4-6]. Peroxydisulfate-O_2, as a novel ECL system, has gradually aroused concern due to its distinct advantages of simplicity, sensitivity and cheapness[7,8]. The mechanisms to the ECL of peroxydisulfate solution are as follows[9].

$$S_2O_8^{2-} + e \rightarrow SO_4^{\bullet -} + SO_4^{2-} \quad (1)$$

$$SO_4^{\bullet -} + H_2O \rightarrow HO^{\bullet} + HSO_4^{-} \quad (2)$$

$$HO^{\bullet} \rightarrow HOO^{\bullet} + H_2O \quad (3)$$

$$O_2 + H_2O + e \rightarrow HOO^{\bullet} + HO^{-} \quad (4)$$

$$SO_4^{\bullet -} + HOO^{\bullet} \rightarrow HSO_4^{-} + {}^1(O_2)_2^{*} \quad (5)$$

$$ {}^1(O_2)_2^{*} \rightarrow 2\,{}^3O_2 + h\nu \quad (6)$$

According to the mechanisms, we know that the dissolved oxygen is a co-reactant of peroxydisulfate. Therefore, the concentration of the dissolved oxygen have directly influence on the ECL signal of peroxydisulfate. However, the sensitivities of some sensors are limited because O_2 as co-reactant is basically from the dissolved oxygen, which suffers from difficulty in labeling and low concentration in the detection solution. Researchers find that in situ generating O_2 is a fascinating method to overcome the above shortages, because many biologically active substances can transform or metabolize to O_2[10]. However, up to date, reports based on ECL of peroxydisulfate using in situ generated O_2 as co-reactant are relatively scarce, especially in aptasensors.

Recently, artificial mimic enzymes, especially catalytic nucleic acids (DNAzymes), have attracted intensive and extensive research interests due to their surprising potential as a new catalytic amplifiers in biosensing events[11,12]. DNAzymes possesses various advantages, such as low cost, easy to label, and more stable against hydrolysis and heat treatment[13]. Hemin/G-quadruplex is an interesting DNAzyme with horseradish

Education Ministry Key Laboratory on Luminescence and Real-Time Analysis, College of Chemistry and Chemical Engineering, Southwest University, Chongqing 400715, People's Republic of China. E-mail: *yuanruo@swu.edu.cn*, *yqchai@swu.edu.cn*; Fax: +86-23-68253172; Tel: +86-23-68252277

peroxidise (HRP) mimicking activities, which consists of hemin intercalated into a single-stranded guanine-rich aptamer[14-16]. Recently, Golub and colleagues reported that the hemin/G-quadruplex could act not only as HRP-mimicking DNAzyme but also as an β-nicotinamide adenine diuncleotide hydrogen (NADH) oxidase[17]. Based on the research achievements above, an amplified TB electrochemical aptasensor was successfully constructed by employing the pseudobienzyme property of hemin/G-quadruplex in our previous work[18]. However, the remarkable catalytic performance of hemin/G-quadruplex has been received little attention in the field of ECL aptasensor.

Gold nanorods (AuNRs), anisotropic and elongated nanoparticles, are of easy preparation, good chemical stability, excellent biocompatibility and fascinating conductivity, have attracted increasing attention in electrochemical biosensors owing to their unique catalytic properties, ease of bioconjugation and large surface area[19-21]. In addition, the surface chemistry of AuNRs is versatile, allowing the linking of various biofunctional groups, like amphiphilic polymers, nucleic acids and proteins, through strong Au-S or Au-N bonding or through physical adsorption [22-24]. And it is worth to be mentioned that AuNRs are normally wrapped with a thin layer of positively charged surfactants, resulting in high stability and positively charged surface. Therefore, AuNRs can easily adsorb many negatively charged biomacromolecules through electrostatic interaction, such as peptide, DNA and even cells[25-28]. Considering these facts, AuNRs have been explored for potential applications in biosensor, photothermal therapy and gene delivery[29-31]. With regards to biosensing applications, Xu and colleagues achieved high sensitivity using a graphene-modified electrode with gold nanorods multilabeled with glucose oxidase and secondary antibody for the ECL immunoassay[32].

In this paper, we prepared a novel and highly sensitive peroxydisulfate ECL aptasensor based on pseudo triple-enzyme cascade catalysis of GDH and hemin/G-quadruplex that simultaneously acts as NADH oxidase as well as HRP-mimicking DNAzyme to generate co-reactant in situ for signal amplification. In this sandwich-type ECL aptasensor, AuNRs constructed an effective platform for loading large amounts of GDH and hemin/G-quadruplex to form secondary aptamer bioconjugate (TBA II) with high stability and bioactivity. AuNRs also worked as a promoter to increase the surface area and accelerate the electron transfer, further amplifying the ECL signal. In the presence of target TB, TBA II was linked to the electrode surface via sandwich reactions. After adding appropriate concentration of glucose and NAD^+ into the ECL detector cell, GDH could effectively catalyze the oxidation of glucose to gluconolatone, coupling with the reduction of NAD^+ into NADH. Then, the hemin/G-quadruplex acted as NADH oxidase, could rapidly oxidize NADH into NAD^+ accompanying with the generation of H_2O_2. Simultaneously, the produced H_2O_2 was further catalyzed by hemin/G-quadruplex which served as the HRP-mimicking DNAzyme to in situ generate O_2, which acted as the co-reactant of peroxydisulfate. Thus, an amplified ECL signal could be obtained through the pseudo triple-enzyme cascade catalysis strategy. The obtained sandwich-type aptasensor exhibited a wide linear range and a low detection limit for TB detection and showed great potential in clinical applications.

Experimental

Materials and reagents

Thrombin (TB), bovine serum albumin (BSA), hemin, gold chloride (HAuCl4), β -nicotinamide adenine dinucleotide hydrate (NAD^+), glucose dehydrogenase (GDH) from pseudomonas ap. were purchased from Sigma (St. Louis, MO, USA). Carcinoembryonic antigen (CEA), α -1-fetoprotein (AFP) and mouse IgG (IgG) were bought from Biocell Company (Zhengzhou, China). $K_2S_2O_8$ was purchased from shanghai chemical Reagent company (Shanghai, China). Hexadecyltrimethylammonium bromides (CTAB), ascorbic acid (AA), $NaBH_4$, $AgNO_3$ were obtained from Kelong Chemical Company (Chengdu, China). Thiol-terminated thrombin binding aptamer (TBA): 5'-SH-$(CH_2)_6$-GGT TGG TGT GGT TGG-3' was obtained from TaKaRa (Dalian. China). Tris-hydroxymethylaminomethane hydrochloride (tris) was purchased from Roche (Switzerland). Serum specimens provided by Daping Hospital of Third Military Medical University (Chongqing, China) were stored at 4 ◦C in a freezer. All other chemicals were of reagent grade and used as received.

Phosphate buffered solution (PBS) (pH 7.4, 0.10 M) were prepared with 0.1 M Na_2HPO_4, 0.1 M KH_2PO_4 and 0.1 M KCl. 20 mM Tris-HCl buffer (pH 7.4) containing 140 mM NaCl, 5 mM KCl and 1 mM $MgCl_2$ was used as a binding buffer. Ferricyanide/ferrocyanide mixed solution ($[Fe(CN)_6]^{3-/4-}$, 5.0 mM, pH 7.4) was employed for CV investigation. Double distilled water was used throughout this study.

Apparatus

The ECL emission was monitored by a model MPI-E electrochemiluminescence analyzer (Xi' an Remax Electronic Science & Technology Co. Ltd., Xi' an, China) Depositions and cyclic voltammetry (CVs) were taken with a CHI 600A electrochemistry workstation (Shanghai CH Instruments, China). A conventional three-electrode system was used with a modified glassy carbon electrode (GCE, Φ = 4 mm) as working electrode, an Ag/AgCl (sat. KCl) as reference electrode and a platinum wire as counter electrode. The morphologies and sizes of nanoparticles were estimated from transmission electron microscopy (TEM, TECNAI 10, Philips Fei Co., Hillsboro, OR). The Ultraviolet-visible (UV-vis) absorption spectrum was recorded with an UV-3600 UV-vis spectrophotometer (Shimadzu, Japan).

Synthesis of Gold Nanorods (AuNRs)

AuNRs were synthesized via a seed-mediated method described in the literature with a little modification[33,34]. Firstly, gold seeds were prepared by adding 0.6 mL freshly prepared ice-cold $NaBH_4$ (0.01 M) to the mixture of 0.25 mL $HAuCl_4$ (10 mM) and 7.5 mL CTAB (100 mM) in a test tube. After strong stirring for 2 min, the seed solution developed a pale brown-yellow color. It was left undisturbed for 2 h at the temperature of 25 ◦C prior of use. Then, the growth solution of the AuNRs was prepared, which contained 40 mL CTAB (100 mM), 1.7 mL $HAuCl_4$•$3H_2O$ (10 mM) and 0.25 mL $AgNO_3$ (10 mM), followed by the addition of 0.27 mL ascorbic acid (100 mM). Finally, 0.42 mL of gold seed solution prepared previously was added to the growth solution, which was

then mixed gently for 10 s and allowed to react in a water bath at 28 ◦C for 18 h. The as prepared AuNRs were purified by centrifugation (8000 rpm, 40 min, 25 ◦C) to remove excess CTAB and finally the precipitates were redispersed in double distilled water. The resulting AuNRs were characterized by transmission electron microscopy (TEM) and UV-Vis spectra (see Electronic Supplementary Information, Fig. S1).

Preparation of secondary aptamer bioconjugate (TBA II)

The process of the preparation of TBA II was shown in the Scheme 1 (A). Firstly, 200 μL thiol-terminated TBA (2.5 μM) was added into prepared AuNRs aqueous solution and stirred for 16 h. Then, the mixture was centrifuged at 12 000 rpm for 30 min to get rid of unbounded TBA and the sediment was resuspended in 2 mL Tris-HCl buffer (pH 7.4). Subsequently, 1.0 mg GDH was put into the mixed solution under softly stirring for about 1 h at 4 ◦C to block the remaining active sites of AuNRs surface. After that, 0.5 mg hemin was added into the above solution with an extra reaction time of 2 h. The finally solution was then subjected to centrifugalization at 12 000 rpm for 30 min and resuspended in 2 mL Tris-HCl buffer and stored at 4 ◦C for the further use.

Fabrication of the sandwich-type electrochemiluminescence aptasensor

The fabrication process for the proposed aptasensor was schematized in Scheme 1 (B). Firstly, glassy carbon electrode (GCE, Φ = 4 mm) was carefully polished with 0.3 and 0.05 μm alumina slurries and sonicated sequentially in water, ethanol and water for 5 min. Then the cleaned electrode was immersed into HAuCl4 solution for electrochemical deposition to obtain a gold nanoparticles (dep-Au) layer. Subsequently, 20 μL TBA (2.0 μM) solution was dropped onto the surface of the dep-Au/GCE surface and incubated for 16 h at room temperature. After that, 20 μL of BSA solution (0.1%) was placed onto the electrode for 40 min to block nonspecific binding sites. The modified electrode was then incubated with 20 μL of various concentrations of TB for 40 min. Lastly, 20 μL of prepared TBA II was put on the TB/BSA/TBA/dep-Au/GCE surface and incubated for 40 min to form sandwich aptasensor. The resulting ECL aptasensor was thoroughly rinsed with Tris-HCl buffer to remove the unbound TBA II on the electrode surface.

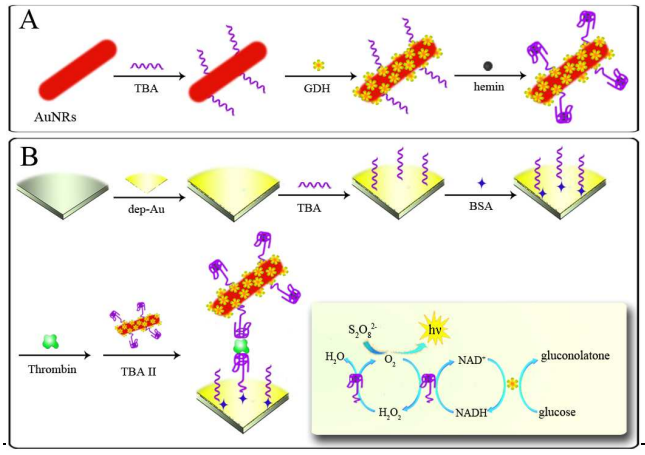

Scheme 1 (A) The preparation procedure of secondary aptamer, (B) Schematic diagram of preparation and reaction mechanism of the ECL aptasensor.

Measurement procedure

Based on the typical process of sandwich format, the obtained aptasensor was incubated with different concentrations of TB solution for 40 min at room temperature. The aptasensor was placed in an ECL detector cell containing 2 mL PBS (pH 7.4) with 0.1 M peroxydisulfate, 0.01 M glucose and an appropriate concentration of NAD^+ to record the change of ECL signals at room temperature. The voltage of the photomultiplier tube (PMT) was set at 800 V and the potential scan from 0 to -2.0 V (vs. Ag/AgCl) with a scan rate of 100 mV s^{-1} in the process of detection. The measurements of clinical serum samples were performed with the same procedures mentioned above without any other treatments.

Results and discussion

CV and ECL behavior of the aptasensor

In order to characterize the fabrication process of the ECL aptasensor, the cyclic voltammetry (CVs) experiments were performed in 5 mM $[Fe(CN)_6]^{3-/4-}$ solution. Fig. 1 (A) showed the CVs of stepwise modified processes of the proposed electrode. A pair of well-defined redox peak of $[Fe(CN)_6]^{3-/4-}$ was observed on the pretreated bare GCE (Fig. 1(A), curve a). When AuNPs were electrodeposited onto the electrode, the current obviously increased (Fig. 1(A), curve b), which ascribed to the enhancement of the effective surface area and the good conductivity of dep-Au layer. When TBA was assembled onto the electrode surface, the current decreased greatly (Fig. 1(A), curve c) due to the inhibitation of the TBA. And the current further decreased (Fig. 1 (A), curve d) after BSA was used to block the possible remaining active sites. Additionally, the introduction of TB induced a decrease of peak current (Fig. 1 (A), curve e) due to the TB could hinder the electrontransfer. Finally, the modified electrode was incubated with TBA II for 40 min, the peak current (Fig. 1 (A), curve f) decreased further.

In this work, ECL analyzer was also used to give detailed information on ECL signal changes during the fabrication process. And all these results were recorded until the electrode had reached a steady-state response. As shown in Fig. 1 (B), a weak ECL signal was observed on the bare GCE (Fig. 1 (B), curve a). The ECL signal was enhanced dramatically when AuNPs were electrodeposited onto the electrode (Fig. 1 (B), curve b), because AuNPs played an important role similar to a conducting wire which made it easier for the electron transfer. However, when TBA was immobilized onto the electrode, an obviously decreased ECL signal was obtained (Fig. 1 (B), curve c). After blocking with BSA, the ECL signal was decreased continuatively (Fig. 1 (B), curve d). The ECL signal further declined after incubated with 10 nM TB (Fig. 1 (B), curve e) for that the protein acted as the inert electron and hindered the electron transfer. A successive decline of ECL signal was detected (Fig. 1 (B), curve f) when the modified electrode was incubated with TBA II.

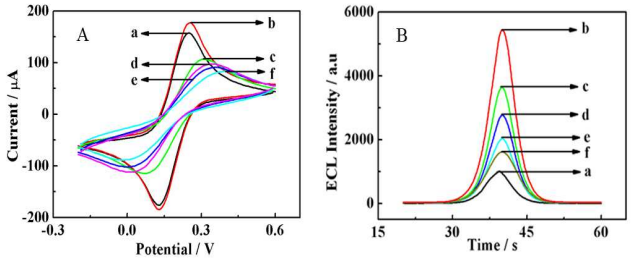

Fig. 1 (A) CVs for (a) bare GCE, (b) dep-Au/GCE, (c) TBA/dep-Au/GCE, (d) BSA/TBA/dep-Au/GCE, (e) TB/BSA/TBA/dep-Au/GCE, (f) TBA Ⅱ/TB/BSA/TBA /dep-Au/GCE in 5.0 mM $[Fe(CN)_6]^{3-/4-}$ (pH 7.4) at scan rate of 100 mV s^{-1}. (B) ECL profiles of (a) bare GCE, (b) dep-Au/GCE, (c) TBA/dep-Au/GCE, (d) BSA/TBA/dep-Au/GCE, (e) TB/BSA/TBA/dep-Au/GCE, (f) TBA Ⅱ/TB/BSA/TBA /dep-Au/GCE in 0.1 M peroxydisulfate solution.

Optimization of analytical conditions

The concentration of NAD^+ is an important factor for the ECL intensity of the aptasensor. Fig. 2 illustrates the ECL signal of the proposed aptasensor at different NAD^+ concentrations when incubated with 10 nM TB. The ECL curves corresponding to different volume of NAD^+ were given in the inset. The change of NAD^+ concentration was gained by adding different volume of NAD^+ into 2 mL PBS (pH 7.4) solution containing 0.01 M glucose. As shown in Fig. 2, the ECL signal enhanced with the increasing of the volume of NAD^+. However, when the volume of NAD^+ reached 120 μL, the ECL intensity increased slowly and tended to reach a constant value. Hence, 120 μL was chosen as the appropriate volume of NAD^+ in this experiment.

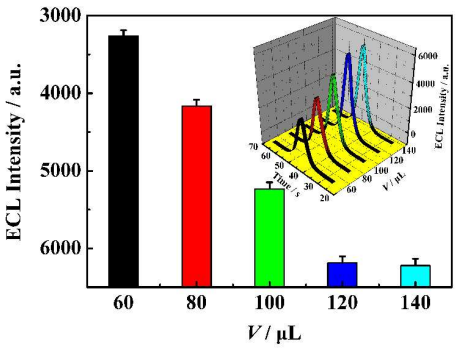

Fig. 2 Effect of the NAD^+ concentration on ECL signals of the proposed aptasensor when incubated with 10 nM TB.

Amplified ECL responses for TB detection

The signal amplification of the proposed aptasensor was based on the catalysis ability of GDH and hemin/G-quadruplex that simultaneously acts as an NADH oxidase as well as HRP-mimicking DNAzyme, and the results were exhibited in Fig.3. As shown, when the proposed aptasensor incubated with 10 nM of TB and 20 μL of TBA II, it showed a small ECL response in 0.1 M peroxydisulfate solution (black curve). After the addition of 0.01 M glucose and 120 μL NAD^+ (0.25 mM) into the ECL detector cell, obvious increase of the ECL response could be observed (red curve). This phenomenon was due to the enzyme catalysis accomplished by the following ways: in the presence of 0.01 M glucose and 120 μL NAD^+ (0.25 mM) into the ECL detector cell, the GDH on the electrode surface could effectively catalyze the oxidation of glucose to gluconolatone, coupling with the reduction of NAD^+ into NADH. Then, the hemin/G-quadruplex firstly acted as NADH oxidase, could rapidly oxidize NADH into NAD^+ accompanying with the generation of H_2O_2. Simultaneously, the produced H_2O_2 was further catalyzed by hemin/G-quadruplex which served as the HRP-mimicking DNAzyme to in situ generate O_2. Then the generated O_2 acted as the co-reactant of peroxydisulfate resulting in a dramatic amplification in the ECL signal.

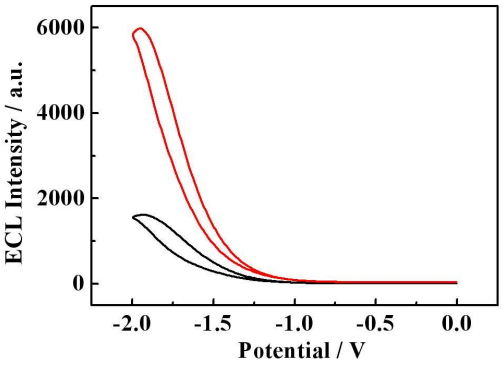

Fig. 3 ECL intensity-potential curves of TBA II/TB/BSA/TBA /dep-Au modified GCE in 0.1 M peroxydisulfate in the absence (black curve) and in the presence of (red curve) 0.01 M glucose and 120 μL NAD^+ (0.25 mM).

ECL detection of TB with the aptasensor

Under the optimized experimental conditions, we explored the quantitative range of the proposed ECL aptasensor by using the developed sandwich-type format. The ECL responses were recorded under continuous scanning to obtain a relative steady ECL signals. As shown in Fig. 4 (A), the ECL signal increased with the increasing concentration of TB in the range from 0.0001 nM to 50 nM. Fig. 4 (B) showed the calibration curve of proposed aptasensor. The linear equation was I_{ECL} = 5633.70 + 509.36 lg (c_{TB}) with a correlation coefficient of 0.998 and an evaluated detection limit of 33 fM (S/N = 3). According to the linear equation, the proposed aptasensor could be applied to detect the concentration of TB quantitatively. As shown in Table S1, the proposed aptasensor exhibited relative wider response range and higher sensitivity compared with previous reported aptasensor (see Electronic Supplementary Information, Table S1).

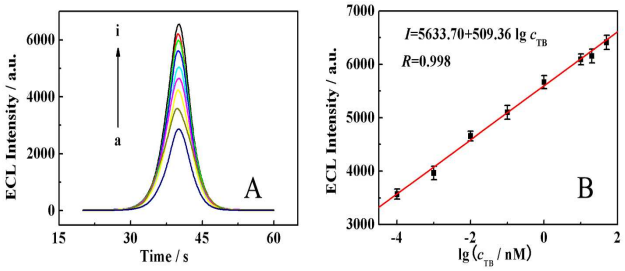

Fig. 4 (A) ECL profiles of the proposed aptasensor to different concentrations of TB (a–i). (B) calibration curve for TB determination. The concentrations of TB: (a) 0 nM, (b) 0.0001 nM, (c) 0.001 nM, (d) 0.01 nM, (e) 0.1 nM, (f) 1.0 nM, (g) 10 nM, (h) 20 nM, (i) 50 nM. All ECL signals were measured in 2 mL PBS (pH 7.4) with 0.1 M peroxydisulfate, 0.01 M glucose and 120 μL NAD^+ (0.25 mM).

Selectivity, stability and reproducibility of the aptasensor

The selectivity of the aptasensor was evaluated by exposing it to other non-target molecules. Therefore, some other proteins such as CEA, AFP, IgG and BSA were examined under the same experiment conditions. As shown in Fig. 5 (A), no apparent change appeared in these ECL signals with interfering substances compared with that of the blank test. However, the presence of target thrombin resulted in a substantial increase in ECL signal. Even when 10-folds concentrations of these interfering substances coexisted with thrombin, no remarkable change of ECL signal was observed in comparison with that in the presence of TB only. These results clearly demonstrated the high specificity and sensitivity of the proposed aptasensor for TB detection.

The stability was also an important factor to assess the performance of the ECL aptasensor. We examined it by employing several aptasensors to detect different concentrations of TB with the use of ECL analyzer. The stability of the ECL signals of this proposed aptasensor to various concentrations of TB is presented in Fig. 5 (B). It showed that the ECL intensity increased with the increasing concentration of TB, and a relative stable curve at every concentration could be obtained.

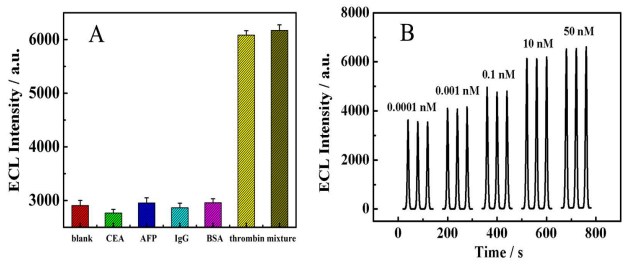

Fig. 5 (A) Selectivity evaluation of the aptasensor against the interference molecules, CEA (100 nM), AFP (100 nM), IgG (100 nM), BSA (100 nM) and their mixing with TB. (B) ECL stability of proposed aptasensor with various concentrations of TB.

The reproducibility of the proposed aptasensor was evaluated by the variation coefficients (ECL signal) of intra- and inter-assays. The intra-assay precision was 5.21%, which was evaluated from the response to 10 nM TB at five different electrodes in the same batch. Similarly, the inter-assay precision was 4.73%, which was assessed by assaying 10 nM TB with five proposed aptasensors made at the same GCE with various batches. Hence, the precision and reproducibility of the proposed aptasensor were acceptable.

Preliminary analysis of real samples

To monitor the feasibility of the developed aptasensors, recovery experiments were performed by standard addition method. A series of samples were obtained by adding thrombin of different concentrations into 10-fold-diluted human serum samples (obtained from Daping Hospital Hospital of Chongqing, China). As shown in Table 1, the recovery (between 93.5% and 110%) was acceptable, which provided a promising alternative tool for determining TB in real biological samples.

Table 1 The recovery of the proposed immunosensor in normal human serum.

Sample	Added thrombin /nM	Found thrombin/nM	Recovery/%
1	0.010	0.011	110
2	0.10	0.098	98.0
3	1.00	1.05	90.5
4	10.0	9.78	97.8
5	20.0	18.7	93.5

Conclusions

In summary, we have successfully constructed a novel and highly sensitive ECL detection method for TB based on pseudo triple-enzyme cascade catalysis of GDH and hemin/G-quadruplex that simultaneously acts as NADH oxidase as well as HRP-mimicking DNAzyme to generate co-reactant in situ. The AuNRs as nanocarrier could load large amounts of GDH and hemin/G-quadruplex, which realized the pseudo triple-enzymtic and progressive amplification of ECL signal. The proposed aptasensor showed high sensitivity, wide linear range, good reproducibility, satisfying precision and accuracy. Thus, this work provided a new method for signal amplification of ECL biosensing and held a promising perspective in the application of peroxydisulfate for high sensitive bioassays.

Acknowledgements

This work was financially supported by the NNSF of China (21275119, 21075100), Ministry of Education of China (Project 708073), Natural Science Foundation of Chongqing City (CSTC-2011BA7003), Specialized Research Fund for the Doctoral

Program of Higher Education (20100182110015) and the Postgraduate Science and Technology Innovation Program of Southwest China University (Grant No. XDJK2012A004, XDJK2013A008).

Notes and references

1 W.J. Miao, Chem. Rev., 2008,108, 2506.
2 B. Paolo and R.J. Forster, Biosens. Bioelectron., 2009, 24, 3191.
3 Y. Chen, Y.Y. Shen, D. Sun, H.Y. Zhang, D.B. Tian, J.R. Zhang and J.J. Zhu, Chem. Commun., 2011, 47, 11733.
4 C.Y. Tian, W.W. Zhao, J. Wang, J.J. Xu and H.Y. Chen, Analyst, 2012,137, 3070.
5 X.F. Tang, D. Zhao and M. N. Zhang, Analyst, 2013,138, 5706.
6 Z.M. Yu, X.H. Wei, J.L. Yan and Y.F. Tu, Analyst, 2012, 137, 1922.
7 H.J. Wang, R. Yuan, Y.L. Chai, H. Niu, Y.L. Cao, X.X. Gan, Y.F. Chen and Y. Wang, Biosens. Bioelectron., 2013, 43, 63.
8 H. Niu, R. Yuan, Y. Chai, L. Mao, H.J. Liu and Y.L. Cao, Biosens. Bioelectron., 2013, 39, 296.
9 W. Yao, L. Wang, H.Y. Wang and X.L. Zhang, Electrochim. Acta, 2008, 54, 733.
10 H. Niu, R. Yuan, Y. Chai, L. Mao, Y.L. Yuan, Y. Zhuo, S.R. Yuan and X. Yang, Biosens. Bioelectron., 2011, 26, 3175.
11 I. Willner, B. Shlyahovsky, M. Zayats and B. Willner, Chem. Soc. Rev., 2008, 37, 1153.
12 Y. Cai, N. Li, D.M. Kong and H.X. Shen, Biosens. Bioelectron., 2013, 49, 312.
13 F.A. Wang, J. Elbaz, R. Orbach, N. Magen and I. Willner, J. Am. Chem. Soc., 2011, 133, 17149.
14 P. Travascio, P. K. Witting, A. G. Mauk and D. Sen, J. Am. Chem. Soc., 2001, 123, 1337.
15 D. J. F. Chinnapen and D. Sen, Biochem., 2002, 41, 5202.
16 Y. Xiao, V. Pavlov, T. Niazov, A. Dishon, M. Kotler and I. Willner, J. Am. Chem. Soc., 2004, 126, 7430.
17 E. Golub, R. Freeman and I. Willner, Angew. Chem. Int. Ed., 2011, 50, 11710.
18 Y.L. Yuan, R. Yuan, Y.Q. Chai, Y. Zhuo, X.Y. Ye, X.X. Gan and L.J. Bai, Chem. Commun., 2012, 48, 4621.
19 H.J. Chen, L. Shao, Q. Li and J.F. Wang, Chem. Soc. Rev., 2013, 42 2679.
20 W. He, Y. Liu, J. Yuan, J.-J. Yin, X.Wu, X. Hu, K. Zhang, J. Liu,C. Chen, Y. Ji and Y. Guo, Biomaterials, 2011, 32, 1139.
21 Z.F. Sun, L. Deng, H. Gan, R.J. Shen, M.H. Yang and Y. Zhang, Biosens. Bioelectron., 2013, 39, 215.
22L. Li, H.M., Lu and L. Deng, Talanta, 2013, 113, 1.
23 D. Du, J. Wang, D.L. Lu, A. Dohnalkova and Y.H. Lin, Anal. Chem., 2011, 83, 6580.
24 S.C. Yan, X. Xu, Y. Sheng, H.B. Sun, J.S. Wu, L.H. Tang and J. Nanosci. Nanotechnol., 2011, 11,10320.
25 P.P. Joshi, S.J. Yoon, W.H. Hardin, S. Emelianov and K.V. Sokolov, Bioconjugate Chem., 2013, 24, 878.
26 W. He, C.Z. Huang, Y.F. Li, J.P. Xie, R.G. Yang, P.F. Zhou and J. Wang, Anal. Chem., 2008, 80, 8424.
27 J.V. Jokerst, A.J. Cole, D.V. Sompel and S.S. Gambhir, ACS Nano, 2012, 6, 10366.
28 A.K. Oyelere, P.C. Chen, X. Huang, I.H. El-Sayed and M.A. El-Sayed, Bioconjugate Chem., 2007, 18, 1490.
29 D.J. Lin, J. Wu, H.X. Ju and F. Yan, Biosens. Bioelectron., 2013, 45, 195.
30 H.T. Ke, J.R. Wang, Z.F. Dai, Y.S. Jin, E.Z. Qu, Z.W. Xing, C.X. Guo, J.B. Liu and X.L. Yue, J. Mater. Chem., 2011, 21, 5561.
31 S.E. Lee, G.L. Liu, F. Kim and L.P. Lee, Nano Letters, 2009, 9, 562.
32 S.J. Xu, Y. Liu, T.H. Wang and J.H. Li, Anal. Chem., 2011, 83, 3817.
33 A. Gole and C.J. Murphy, Chem. Mater., 2004, 16, 3633.
34 W. Li, J.S. Wang, J.S. Ren and X.G. Qu, Angew. Chem. Int. Ed. 2013, 52, 6726.